

# Spin-dependent resonant tunneling through quantum-well states in magnetic metallic thin films \*

Zhong-Yi Lu and X.-G. Zhang

*Computer Science and Mathematics Division,  
Oak Ridge National Laboratory, Oak Ridge, TN 37831*

Socrates T. Pantelides

*Dept. of Physics and Astronomy, Vanderbilt University, Nashville, TN 37235  
and Oak Ridge National Laboratory, Oak Ridge, TN 37831*

(Dated: November 14, 2018)

## Abstract

Quantum-well (QW) states in *nonmagnetic* metal layers contained in magnetic multilayers are known to be important in spin-dependent transport, but the role of QW states in *magnetic* layers remains elusive. Here we identify the conditions and mechanisms for resonant tunneling through QW states in magnetic layers and determine candidate structures. We report first-principles calculations of spin-dependent transport in epitaxial Fe/MgO/FeO/Fe/Cr and Co/MgO/Fe/Cr tunnel junctions. We demonstrate the formation of sharp QW states in the Fe layer and show discrete conductance jumps as the QW states enter the transport window with increasing bias. At resonance, the current increases by one to two orders of magnitude. The tunneling magnetoresistance ratio is several times larger than in simple spin tunnel junctions and is positive (negative) for majority- (minority-) spin resonances, with a large asymmetry between positive and negative biases. The results can serve as the basis for novel spintronic devices.

PACS numbers: 85.75.Mm, 73.40.Rw, 75.47.Jn

---

\* The submitted manuscript has been authored by a contractor of the U.S. Government under contract No. DE-AC05-00OR22725. Accordingly, the U.S. Government retains a nonexclusive, royalty-free license to publish or reproduce the published form of this contribution, or allow others to do so, for U.S. Government purposes.

Metallic QW states have long been known to play an important role in spin-dependent transport. Recently, Yuasa *et al*<sup>1</sup> observed oscillations of the tunneling magnetoresistance ratio (TMR) in Co/Cu/Al-O/Ni-Fe tunnel junctions as a function of the thickness of the Cu layer, demonstrating the effect of quantum confinement of electrons in the nonmagnetic Cu layer. Most studies, however, have focused on QW states in a *nonmagnetic* layer incorporated in a magnetic multilayer structure. In these nonmagnetic layers, the electron energy dispersion is close to that of a free electron, QW states can easily be identified, and simple models can be readily applied. There exists only one report of an experimental attempt to explore spin-dependent transport through confined *magnetic* thin films. In 2002, Nagahama *et al* reported<sup>2</sup> indications of oscillations in the tunneling conductance of a (100) Cr/Fe/Al-O/FeCo tunneling junction, where QW states were expected to be present in the magnetic Fe layer. The observed effect was very small, seen only in the second derivative of the current-voltage curve. Yuasa *et al*<sup>1</sup> attributed the smallness of the effect to the short mean free path and spin diffusion length in Fe. Resonant tunneling through QW states in magnetic thin films is worth exploring further, however. In addition to the intrinsic interest, resonant tunneling through magnetic layers can be switched on and off by external magnetic fields, which offers additional control in designing spintronics devices.

In this paper, we first discuss several factors that may have contributed to the smallness of the effect observed in Ref. 2. We then identify criteria which, when met by candidate structures containing a magnetic thin film, ensure the formation of sharp QW states in the magnetic film and result in strong resonant tunneling. We use these criteria to select specific structures for a detailed theoretical study. We report results of first-principles calculations of spin-dependent transport through select structures (bcc (100) Fe/MgO/FeO/Fe/Cr and Co/MgO/Fe/Cr with epitaxial lattices) and analyse the results. We first demonstrate the existence of sharp QW states in the thin Fe layer and then demonstrate that resonant tunneling occurs through these states as the bias increases gradually. At resonance, the current increases by one to two orders of magnitude and the tunneling magnetoresistance ratio (TMR) increases by several orders of magnitude. The resonances are asymmetric with respect to positive or negative biases. By analysing the wave functions of QW states, we demonstrate that the series of resonances observed in Ref. 2 as a function of the Fe film thickness are from *different* QW states that sequentially enter and leave the energy window under analysis. Finally, we show that a previously unknown QW state in the Fe minority spin channel contributes to a large and negative TMR.

We start with a discussion of the experimental data of Ref. 2. The smallness of the observed

effect is likely to be caused by several factors. One factor is the amorphous nature of the Al-O barrier layer, which results in an atomically rough interface (Si/SiO<sub>2</sub> is the most abrupt known crystal-amorphous interface, but it has roughness of order 1-2 monolayers<sup>3</sup>). The roughness causes smearing of the energy width of possible QW states, which reduces resonant-tunnelling effects. A short spin mean free path and diffusion length is a possible second factor, as mentioned in Ref. 1. Indeed, it has been found<sup>4</sup> that in thin Fe (100) films grown epitaxially on a GaAs substrate, the majority spin mean-free-path is about 1.1 nm. The resonance effects based on majority-spin QW states would then be limited to Fe films that are thinner than about 1 nm. However, the minority spin mean free path is much larger, about 14 nm. If we assume that the spin diffusion length is comparable, pronounced QW effects from the minority spin channel should be more readily observable than from the majority spin channel in Fe (100) films of practical thicknesses. There exists a third factor that can play an important role. The energy bands in the magnetic film, the spacer layer, and the electrodes, especially their band offsets at the interfaces, control the formation of QW states while the Bloch-function symmetries control the transmission coefficient and hence the magnitude of the resonant tunneling current. This point was demonstrated in Refs. 5,6,7,8, where the existence of  $\Delta_1$  Bloch states near the Fermi energy is an essential feature of large TMRs in FM1/MgO/FM2 tunnel junctions, where FM1 and FM2 stand for either Fe or Co. In such systems, distinct differences between the two spin channels, and any possible sharp resonances arise from the precise matching or mismatching of the Bloch wave function symmetries on both sides of the barrier. Resonant tunneling is then predicated on having a ballistic tunnel junction. From this point of view, the amorphous nature of the barrier layer may be the critical factor that suppressed resonant tunneling in the experiments of Ref. 2.

The above analysis leads to two criteria for the selection of candidate structures. First is the use of a crystalline spacer layer in a structure consisting of crystalline epitaxial layers. One obvious choice is MgO, which has already been used in both theoretical and experimental<sup>9,10,11</sup> work in simple spin tunnel junctions, as mentioned earlier. Lattice-matching considerations automatically limit the choice of metal layers to the bcc solids of the 3d transition metal series and the orientation of the layers to the (100) direction. The second criterion is the suitability of the energy bands and band offsets of the thin films and electrodes. The electrode in direct contact with the thin magnetic film must be nonmagnetic while the other electrode, separated by the MgO spacer, must be magnetic. To accentuate the resonance effect through the tunneling process, the QW states must be produced from a band at the Fermi energy. The symmetry of the band must match the

complex band structure in the energy gap of MgO so that the QW states have a higher transmission amplitude through the tunnel barrier than states with a different symmetry. For the bcc solids in the (100) direction with the MgO as the barrier, the relevant band has  $\Delta_1$  symmetry. The confinement effect can only be produced if in the nonmagnetic electrode the bottom of the  $\Delta_1$  band is well above the Fermi energy.

Based on the above criteria, the magnetic film and the magnetic electrode can be either bcc Fe or bcc Co. The nonmagnetic electrode must be bcc Cr. The minority-spin band structure of bcc Fe is very similar to bcc Cr, while the majority spin has a very different band structure than Cr.<sup>14</sup> Along the symmetry axis  $\Gamma H$ , the Fe majority-spin  $\Delta_1$  band crosses the Fermi energy, but there is no  $\Delta_1$  band near the Fermi energy for either the Fe minority spin nor the Cr band structure. In addition to the band offsets needed for producing QW states, these energy-band features provide a differentiation between the two spin channels, which we will exploit in order to achieve strong spin-dependence in the resonant tunneling effect.

Using Fe as the magnetic film and the magnetic electrode, our first model system is the bcc (100) Fe/MgO/FeO/Fe/Cr junction. Here we assume that the Cr electrode is deposited first, so that the junction contains a single atomic layer of FeO at the bottom interface between Fe and MgO, which is observed experimentally<sup>12,13</sup> and was shown<sup>6</sup> to greatly impact the TMR. The structure is similar to the tunnel junctions measured in Ref. 2, except for the barrier layer which was Al-O. In our second model system, we use Co as the magnetic electrode, and assume that the Co electrode is deposited first, which produces bcc (100) Co/MgO/Fe/Cr. Unlike the first system, there has not been clear experimental evidence of an oxide layer between the Co electrodes and the barrier MgO layer.

Epitaxial ultrathin films are pseudomorphic, which allows us to fix all bcc Fe, Co, and Cr lattice constant of 2.86 Å, corresponding to that of bulk Fe. The MgO lattice constant is taken to be a factor of  $\sqrt{2}$  larger than that of the bulk electrodes, so that the (100) layers of all the materials can be matched epitaxially. We assumed no vertical relaxations between the layers. All calculations were performed using the layer-KKR implementation<sup>16</sup> of the local-spin density approximation (LSDA) of density functional theory. The self-consistent calculations at zero bias were performed in the same manner as in Refs. 5,6,7. In all calculations, the thickness of the MgO layer is fixed at eight atomic layers. Although the ground state of Cr is antiferromagnetic, for simplicity of the calculation we assumed that the bulk part of the Cr electrode is nonmagnetic. The moments of five Cr layers next to the QW layer were allowed to relax and they showed small moments with

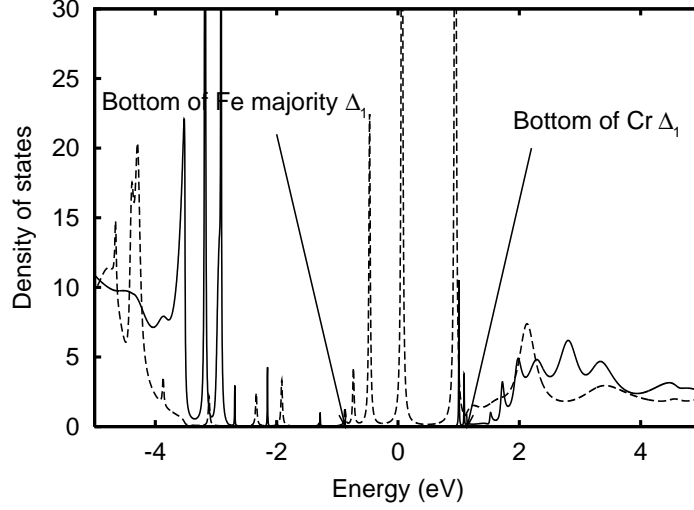


FIG. 1:  $s$ -resolved partial density of states in the eight Fe layers in the QW film of the Fe/MgO/FeO/8Fe/Cr junction at the  $\bar{\Gamma}$  ( $k_{\parallel} = 0$ ) point. Solid line: minority spin, dashed line: majority spin. The Fermi energy is at 0 eV.

alternating signs. The self-consistent charge as a function of bias and the current-voltage curves are calculated following the procedure in Ref. 15.

At the  $\bar{\Gamma}$  point, the  $\Delta_1$  band is primarily  $s$  (angular momentum  $l = 0$ ) but there is no  $s$  component in any of the other bands. In Fig. 1, we show the  $s$  partial DOS within the Fe film sandwiched between the MgO barrier layer and the Cr layer in bcc (100) Fe/MgO/FeO/8Fe/Cr, with an eight monolayer (ML) thickness of the Fe film. There is a gap around the Fermi energy with the bottom of the conduction band coming from the tail of the  $\Delta_1$  band in the Cr electrode. Within this gap, there are several QW states as indicated by the sharp spikes in the DOS. In the majority-spin channel, five of these states are above the Fe majority  $\Delta_1$  band bottom and are derived from the majority  $\Delta_1$  band. The width of these peaks equals to exactly twice the imaginary part of the energy and scales linearly as the imaginary part of the energy. This gives us confidence that the true width of these states is essentially zero, and that they are indeed QW states and not resonances.

The surprise in Fig. 1 is the unexpected QW state for the minority spin. This is not an interface state since its wave function extends throughout the Fe film. The minority spin  $\Delta_1$  band bottom of bcc Fe is above the Fermi energy and is above the  $\Delta_1$  bottom of nonmagnetic bcc Cr at the same lattice constant when the Fermi energy in both solids are aligned. The possible reason that a  $\Delta_1$  QW state may form here is the the relative shifts of the atomic potentials on both sides of the interface in the ultrathin film likely to be different than those of bulk bcc solids. However, this

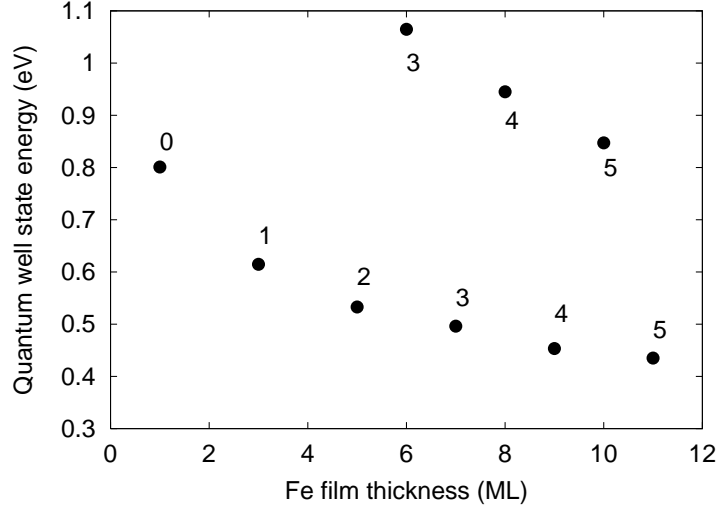


FIG. 2: The thickness dependence of the majority spin QW state energies for Fe/MgO/FeO/ $n$ Fe/Cr for  $n = 1, \dots, 11$ . The numbers next to the data points indicate the number of nodes in the wave function.

QW state is not seen in the Co/MgO/9Fe/Cr junction, indicating that it is probably sensitive to the presence (or absence) of the FeO layer on the interface.

The thickness dependence of the majority spin QW state energies relative to the Fermi energy is shown in Fig. 2 for QW states between 0.3 eV and 1.1 eV. This window is the same as the one in which Nagahama et al<sup>2</sup> observed oscillations in conductance due to the QW states. If we compare Fig. 2 with Fig. 2 in Ref. 2, the agreement between the two figures is striking. However, the differences between the two figures are more important because they tell us what we cannot learn from experimental data alone. We note that in Ref. 2 a QW resonance is observed at each monolayer thickness. This observation led to the assumption that each series of resonances is due to the same QW state. The dispersion deduced from this assumption does not fit any known QW states in Fe(100) films, which led the authors to conjecture that the resonances are due to QW states from the  $\bar{X}$  point rather than the  $\bar{\Gamma}$  point. In contrast, in Fig. 2, the lower resonances occur within this energy window for odd layer thickness only, while the higher resonances occur for even layer thickness only. Analysis of the wave functions reveals that each series corresponds to a number of different QW states, all from the  $\bar{\Gamma}$  point. The numbers next to each data point in Fig. 2 indicate the number of nodes of the wave function. This picture tells us that, when the layer thickness increases by 1 or 2 ML, one QW state moves out of the energy window and the next QW state moves in. Ref. 2 observed QW resonances at about the same bias voltage for both even and odd layers. The actual films in that experiment may consist of regions of varying thicknesses.

In Fig. 3 we show the calculated I-V curves of the Fe/MgO/FeO/8Fe/Cr, (a), and Co/MgO/9Fe/Cr, (b), tunnel junctions for both spin channels with the moment in the Fe film aligned parallel or antiparallel to the Fe (or Co) electrode. A positive bias is defined to make the Fermi energy of the Cr electrode higher than that of the ferromagnetic electrode on the other side of the tunnel barrier. For positive biases, electrons are injected into the QW states and states above the Fermi energy are important. Likewise for negative biases the QW states below the Fermi energy are important. The tunneling current for the majority-spin channel shows a staircase feature where the sharp jumps in the current occur at bias voltages that are precisely equal to the energies of the QW states. Between these resonances, the current remains nearly constant. This result indicates that nearly all of the majority-spin current flows through the QW states. The first QW resonance for Fe/MgO/FeO/8Fe/Cr at positive biases occurs at 0.068 V. At this voltage, the tunneling current increases by more than an order of magnitude. The first resonance for Co/MgO/9Fe/Cr is at 0.238 V, where the tunneling current shoots up by two orders of magnitude. The jumps in the tunneling current for negative biases at the same voltage values are smaller. At low biases, there are no dramatic jumps in the tunneling current for antiparallel alignment of the moments (the moment of the Fe film is aligned oppositely with respect to that of the Fe electrode). Thus, the resonance effect can be easily switched off by applying a small magnetic field. For the Fe/MgO/FeO/8Fe/Cr junction, the antiparallel current becomes larger by almost an order of magnitude than the parallel current when the positive bias approaches 1 volt. At this voltage, the QW state in the Fe minority-spin channel enters the transport window, resulting in a large negative TMR, as we will see below. Such effect is not seen for the Co/MgO/9Fe/Cr junction.

In Fig. 4 we show the conductance ratio  $G_P/G_{AP}$ , where  $G_P$  is the parallel conductance and  $G_{AP}$  is the antiparallel conductance, as a function of the bias voltage for the same tunnel junctions. At very small voltages the TMR is sharply negative ( $G_P/G_{AP} < 1$ ). For Fe/MgO/FeO/8Fe/Cr the ratio  $G_{AP}/G_P$  approaches 1600% near zero bias. Because one of the electrodes is Cr, which does not have the  $\Delta_1$  state near the Fermi energy, the majority-spin tunneling current is suppressed at small biases when the QW states are outside the bias window producing the negative TMR. The TMR reaches peaks at the voltages when each additional QW state starts to contribute to the tunneling current. The effect is particularly large for positive biases. For the Fe/MgO/FeO/8Fe/Cr junction, the first QW resonance at positive biases produces a maximum TMR of 1200%. This value is an order of magnitude larger than the calculated TMR<sup>15</sup> obtained at this voltage for a similar junction but with Fe electrodes on both sides, whereby the QW states were absent. For the

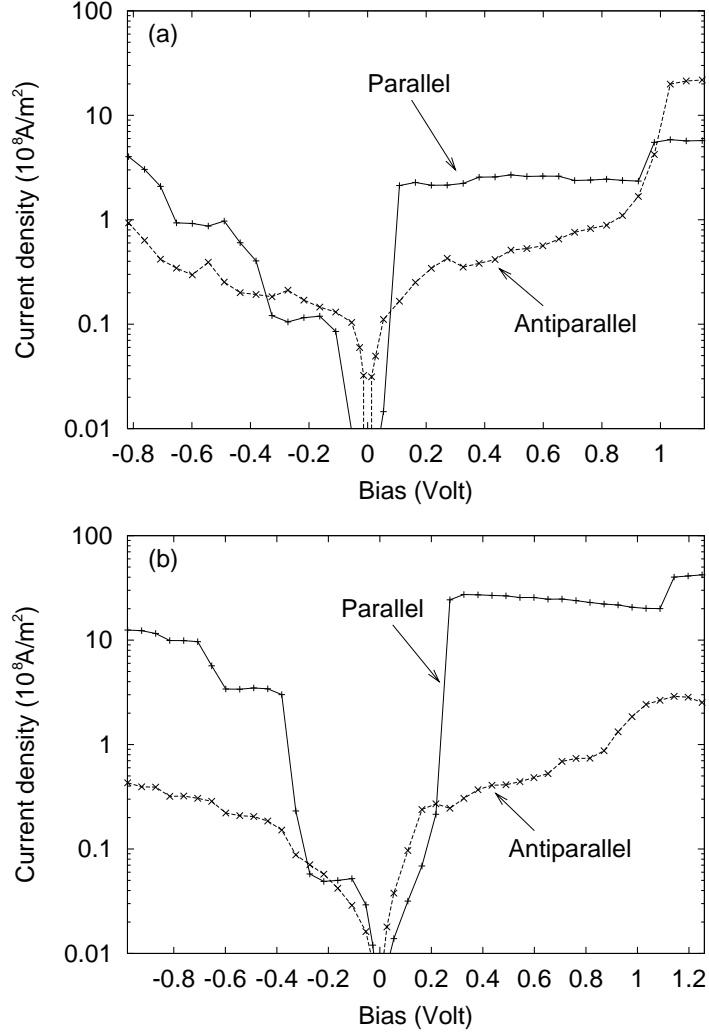


FIG. 3: Tunneling current as a function of bias voltage. (a) Fe/MgO/FeO/8Fe/Cr, (b) and Co/MgO/9Fe/Cr. Solid lines are for parallel alignment of the moments in the Fe film with the magnetic electrode. Dashed lines are for antiparallel alignment.

Co/MgO/9Fe/Cr junction, the maximum TMR reaches 10000%. At higher bias, the TMR declines with voltage because the resonant contribution from each QW state remains relatively constant while the antiparallel current increases with the voltage. For the Fe/MgO/FeO/8Fe/Cr junction, the minority spin QW resonance appears near 1 volt and the TMR turns negative again at this bias. Above 1 volt the ratio  $G_{AP}/G_P$  is 380% .

To summarize, our first-principles calculations predict a significant QW resonance effect in a class of tunneling junctions including Fe/MgO/FeO/Fe/Cr and Co/MgO/Fe/Cr. We predict several-fold increases in tunneling current and the TMR due to resonant tunneling through the metallic

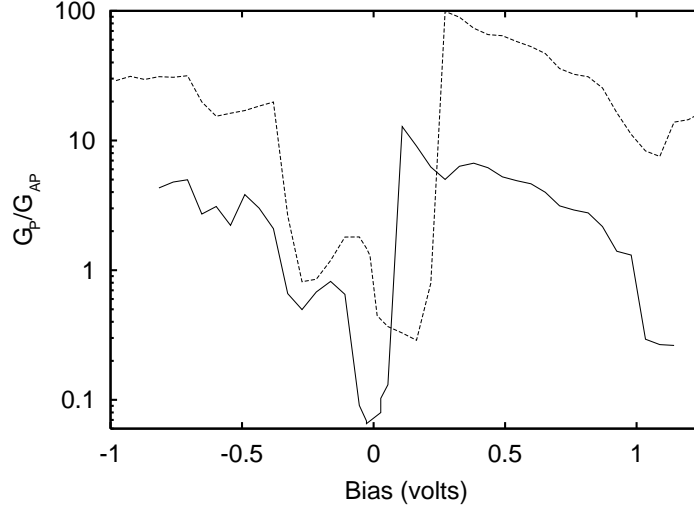


FIG. 4: Conductance ratio as a function of bias voltage for Fe/MgO/FeO/8Fe/Cr (solid line) and Co/MgO/9Fe/Cr (dashed line).

QW states in the Fe film. Both majority and minority spin QW states can contribute to resonant tunneling. The former contributes positively to the TMR while the latter negatively. We also predict a large asymmetry in the I-V curve between positive and negative biases. These properties make these junctions excellent candidates for novel spintronics devices that may combine the features of diodes, rectifiers, field effect transistors, and TMR sensors.

This work was supported by the Office of BES Division of Materials Sciences, and the Office of ASCR Division of Mathematical, Information and Computational Sciences of the U.S. DOE. Oak Ridge National Laboratory is operated by UT-Battelle, LLC, for the U.S. DOE under contract DE-AC05-00OR22725. The work was further supported by the DOE grant FDEFG0203ER46096, and by the McMinn Endowment at Vanderbilt University.

---

<sup>1</sup> S. Yuasa, T. Nagahama, and Y. Suzuki, *Science* **297**, 234 (2002).

<sup>2</sup> T. Nagahama, S. Yuasa, Y. Suzuki, and E. Tamur, *J. Appl. Phys.* **91**, 7035 (2002).

<sup>3</sup> A. Bongiorno, A. Pasquarello, M. S. Hybertsen, and L.C. Feldman, *Phys. Rev. Lett* **90**, 186101 (2003).

<sup>4</sup> A. Enders, T. L. Monchesky, K. Myrtle, R. Urban, B. Heinrich J. Kirschner, X.-G. Zhang and W. H. Butler, *J. Appl. Phys.* **89**, 7110 (2001).

<sup>5</sup> W. H. Butler, X.-G. Zhang, T. C. Schulthess, and J. M. MacLaren, *Phys. Rev. B* **63**, 054416 (2001).

- <sup>6</sup> X.-G. Zhang, W. H. Butler, and Amrit Bandyopadhyay, *Phys. Rev. B* **68**, 092402 (2003).
- <sup>7</sup> X.-G. Zhang and W. H. Butler, *Phys. Rev. B*, manuscript number LQ9658BJ, accepted.
- <sup>8</sup> J. Mathon and A. Umerski, *Phys. Rev. B* **63**, 220403(R) (2001).
- <sup>9</sup> S. Yuasa, A. Fukushima, T. Nagahama, K. Ando, and Y. Suzuki, *Jap. J. Appl. Phys.* **43**, L588 (2004).
- <sup>10</sup> X. Jiang, *Bulletin of APS*, **49** 1079, (2003). R. Wang, X. Jiang, R. Shelby, R. MacFarlane, S. Bank, J. Harris, S. Parkin, *Bulletin of APS* **49** 1079 (2003).
- <sup>11</sup> S. S.P. Parkin, C. Kaiser, A. Panchula, P. Rice, B. Hughes, M. Samant, and S.-H. Yang, preprint.
- <sup>12</sup> H. L. Meyerheim, R. Popescu, J. Kirschner, N. Jedrecy, M. Sauvage-Simkin, B. Heinrich, and R. Pinchaux, *Phys. Rev. Lett.* **87**, 076102 (2001).
- <sup>13</sup> H. L. Meyerheim, R. Popescu, N. Jedrecy, M. Vedpathak, M. Sauvage-Simkin, R. Pinchaux, B. Heinrich, and J. Kirschner, *Phys. Rev. B* **65**, 144433 (2002).
- <sup>14</sup> V. L. Moruzzi, J. F. Janak, and A. R. Williams, *Calculated Electronic Properties of Metals*, (Pergamon, New York, 1978).
- <sup>15</sup> C. Zhang, X.-G. Zhang, P. S. Krstić, H.-P. Cheng, W. H. Butler, and J. M. MacLaren, *Phys. Rev. B* **69**, 134406 (2004).
- <sup>16</sup> J. M. MacLaren, X.-G. Zhang, W. H. Butler, and Xindong Wang, *Phys. Rev. B* **59**, 5470 (1999).